

---

## Chapter 20

# Fundamental aspects of air breakdown

N.L. Allen

---

### 20.1 Introduction

In almost all cases where we are dealing with the dielectric breakdown of air, we are concerned with electric fields which are highly nonuniform. It is characteristic of such breakdowns that the final sparkover is preceded by streamer formation, followed in many cases by a 'leader' which develops prior to the breakdown itself. These processes are known to occur under impulse overvoltages, and under alternating and direct voltages. Before discussing the breakdown characteristics themselves, a brief explanation of the preceding processes is given, since the former are largely determined by the latter.

### 20.2 Pre-breakdown discharges

A description is best given, initially, in terms of an impulse overvoltage applied to an electrode system in which the electrodes have sharp radii, giving rise to large electric fields. Near the positive electrode, ionising electron collisions in the air may form avalanches sufficiently large to create a streamer system – this is a corona which spreads out like a fan from the electrode (Figure 20.1). The streamers propagate with a velocity  $> 10^5 \text{ ms}^{-1}$  and it is known that the electric gradient in the streamer channel is of the order of  $500 \text{ kVm}^{-1}$ . Once the corona is formed, further development is 'choked off' for a period up to a few tens of microseconds by its own space charge, which reduces the electric field near the electrode, but in the prevailing electric field some heating, which can be envisaged as ohmic heating ( $I^2R$ ), takes place in the very resistive channel. This results in a rise in temperature, a decrease in gas density and

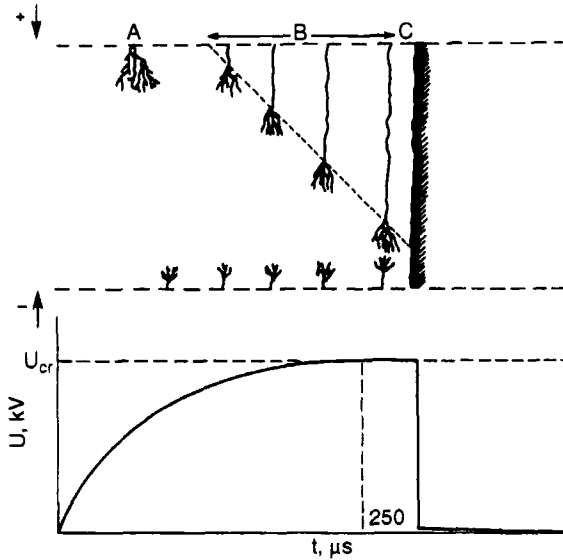


Figure 20.1 Time-extended picture of pre-breakdown corona and sparkover in a system with highly stressed positive and negative electrodes, e.g. the rod-rod gap. Impulse voltage reaching crest  $V_{cr}$  at time  $T_{cr} = 250 \mu s$ . A - initial streamer corona; B - leader growth phase; C - breakdown

increased ionisation, so fostering the transition to an arc-like leader channel which, starting at the electrode, extends across the gap at the relatively low velocity of  $\approx 10^4 \text{ ms}^{-1}$ . This channel is highly conducting with a low electric gradient and, in a simple picture, can be regarded as an extension of the anode across the gap. More streamers thus propagate from the tip of the advancing leader. Figure 20.1 shows a time-extended picture of these events for an impulse reaching crest in, for example, 250  $\mu s$ .

Avalanches, resulting in streamer formation, also occur at the cathode, but here electrons advance into regions of reducing field. The regions of ionisation are less extensive and require a higher electric gradient, of the order of  $1000 \text{ kV m}^{-1}$  for streamer propagation. The negative corona is, in general, much less extensive than the positive corona.

Sparkover occurs after a conducting channel is established across the gap, that is, when the respective ionisation zones meet. The voltage at which breakdown occurs can then be quantified in the following way:

Let  $E_s^+, E_s^-, l_s^+, l_s^-$  be the gradients and lengths of positive and negative streamers, respectively, at the instant of breakdown.  $E_l^+, E_l^-, l_l^+, l_l^-$  are the corresponding quantities for the positive and negative leaders. The voltage  $V_s$  at breakdown for a gap spacing  $d$  is

$$V_s = E_l^+ l_l^+ + E_s^+ l_s^+ + E_l^- l_l^- + E_s^- l_s^- \tag{20.1}$$

Also,

$$d = l_l^+ + l_s^+ + l_l^- + l_s^- \quad (20.2)$$

In most electrode configurations, the lengths  $l$  are unknown, though the gradients are known or can be estimated. However, there is a useful simplification with the rod-plane electrode system where, since the negative electrode is only lightly stressed with a nearly uniform electric field,  $l_l^- = l_s^- = 0$ . Thus, from eqns (20.1) and (20.2), eliminating  $l_s^+$ :

$$V_s = E_s^+ d - l_l^+(E_s^+ - E_l^+) \quad (20.3)$$

Comparison of eqns (20.1) and (20.3) makes it clear that, where there is no negative corona, as in the rod-plane case,  $V_s$  is lower than it would have been in a gap where a significant negative corona occurred, as in the case where two highly stressed electrodes are used. Thus, the rod-plane gap exhibits the lowest sparkover gradient of any nonuniform field gap, and this property forms a useful reference with which other gaps are compared.

### 20.3 The 'U-curve'

From the foregoing description of the growth rates of streamers and leaders, it follows that the sparkover voltage of a gap depends on the rate of rise of voltage in an impulse and on the electrode spacing. These dependences are manifest in the existence of the so-called 'U-curves'. For a fixed electrode spacing, the sparkover voltage, plotted as a function of impulse time-to-crest, passes through a clearly defined minimum. There is a different U-curve for each electrode spacing, with the minimum (known as the 'critical time to crest'  $T_{crit}$ ) occurring at larger times-to-crest as the spacing increases. Examples for the rod-plane gaps are shown in Figure 20.2 [1].

The characteristic profile of the U-curve arises because the leader, which advances at a velocity which varies little with voltage, is able to extend further into the gap as the time-to-crest voltage increases from a small value. For example, taking the rod-plane gap as the simplest case, where a lightning impulse is applied rising to crest in the order of 1  $\mu$ s, there is little time for more than rudimentary leader growth after a streamer corona has occurred (usually on the wavefront), and in eqn (20.3), the second term is negligible, so that

$$V_s = E_s^+ d \quad (20.4)$$

Since  $E_s^+$  has a constant value of  $\approx 500$   $\text{kV m}^{-1}$ , regardless of streamer

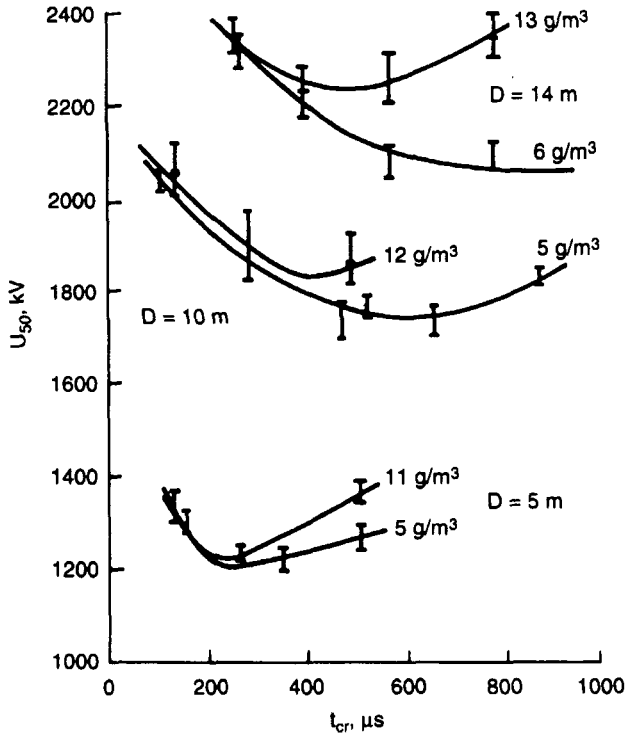


Figure 20.2  $U$ -curves obtained with impulse voltages of various times-to-crest applied to rod-plane gaps. Atmospheric humidity varied in these experiments (see Section 20.6.1 [1])

length, the positive sparkover voltage varies linearly with electrode spacing, a result that has been confirmed by experiments with electrode spacings up to 6 m [2]; see Figure 20.3.

For longer times-to-crest, the leader, with associated streamers, has more time to advance across the gap. Since its gradient  $E_l^+$  is relatively small (and decreasing, in fact, with  $l_l^+$ ) [3], inspection of eqn (20.3) shows that  $V_s < E_s^+d$ . More detailed investigation shows that  $V_s$  decreases with increasing time-to-crest and a minimum value is reached at  $T_{crit}$ , when optimum leader development occurs.

Where the impulse has a time-to-crest  $>T_{crit}$ , that is, with a low rate of rise of voltage, formation of the leader may be preceded by several streamer coronas, so reducing the electric field near the positive electrode and inhibiting the ohmic heating of the streamer channels. Leader formation then requires higher total voltages, and the value of  $V_s$  tends to increase. Thus a minimum occurs in the  $V_s$ /time-to-crest characteristic.

Further consideration of the effects summarised in eqns (20.1) and (20.3) will show that the value of  $T_{crit}$  increases with the electrode spacing  $d$ .

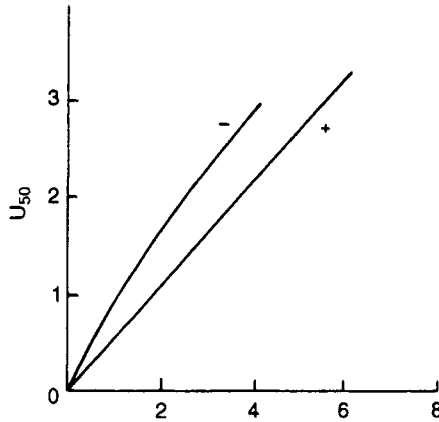


Figure 20.3 Positive and negative lightning impulse sparkover characteristics for rod-plane gaps (after [2])

## 20.4 The gap factor

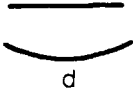
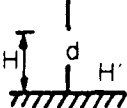
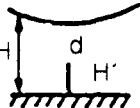
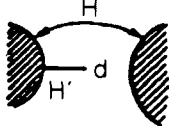
This is a rule-of-thumb used for estimating the sparkover voltages of gaps of various geometries, based on the sparkover voltage of a rod-plane gap of the same length. Again, this is discussed in terms of sparkover under positive impulse voltage in the first instance.

Eqn (20.1) indicates that the sparkover voltage depends on the spatial extent of corona at the electrodes; this in turn depends on the nature of the electric field in the vicinity of the electrodes and hence on their geometry. This has given rise to the concept of the 'gap factor', which is defined as the ratio of the sparkover voltage for a given electrode configuration to that for the rod-plane gap which, as we have seen, exhibits the smallest flashover voltage for a given electrode separation and can be taken as a reference. Tables 20.1 and 20.2, reproduced from the work of Hutzler *et al.* [4], show values of gap factor  $K$  that have been derived by experiment, together with empirical formulae for the calculation of their values.

It is, however, necessary to use the concept with caution. Returning to the growth characteristics for streamers and leaders, we see that an electric field near a stressed electrode will, depending on its shape, determine the extent of the streamer growth and consequent leader initiation. Progress to breakdown thus depends on combined effects due to the time-to-crest voltage and the electric field distribution. The  $U$ -curve of the electrode system under consideration and that of the rod-plane gap will thus not be linked by a simple proportionality; in other words, the gap factor will vary with the waveshape.

As an example, the  $U$ -curves for 13 m positive conductor-plane,

Table 20.1 Gap factors of a number of basic configurations. If  $k > 1.6$ , withstand in negative polarity is less than in positive

Configuration		k
Rod-plane		1
Conductor-plane		1.1 to 1.15
Rod-rod		$1 + 0.6 \frac{H'}{H}$
Conductor-rod		$(1.1 \text{ to } 1.15) \exp\left(0.7 \frac{H'}{H}\right)$
Protuberances		$k_0 \exp\left(\pm 0.7 \frac{H'}{H}\right)^*$ $k \geq 1$

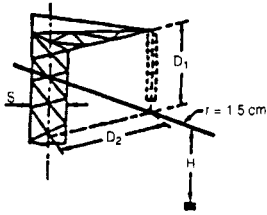
\* Sign + for protuberances at the negative electrode  
Sign - for protuberances at the positive electrode

sphere-plane and rod-plane gaps are presented in Figure 20.4, together with gap factors calculated from the curves. These show significant variations with time-to-crest over a range of switching impulses [4].

Again, for the specific example of the vertical rod-rod gap, the gap factor depends on the height of the tip of the 'earthy' rod above the ground plane. Figure 20.5 shows results obtained from the sparkover characteristics of a rod-rod gap of electrode spacing  $d$  in which the height above ground  $h$  of the tip of the rod was progressively increased while keeping the ratio  $h/d$  constant [5]. The gap factor gradually increases as the height of the gap above ground level increases. This is the result of changes in the disturbing effect of the ground plane on the electric field distribution in the gap. Under lightning impulse, gap factors tend to be smaller than under switching impulse. This is a consequence of the small amount of leader development [6]. Nevertheless, the proximity of earthed metal surfaces can, again, exert a considerable effect on the

Table 20.2 Experimentally derived gap factor  $K$  [4]

Sketch of the configuration & conductor cross-arms

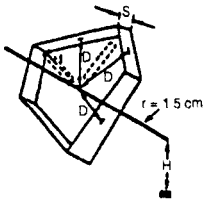


$$K = 1.45 + 0.015 \left( \frac{H}{D} - 6 \right) + 0.35 (e^{-8 S/D} - 0.21) + 0.135 \left( \frac{D_2}{D_1} - 1.5 \right) \quad K = 1.45$$

Applicable in the range:

$$D_1 = 2 + 10 \text{ m} \quad D_2/D_1 = 1 + 2 \\ S/D_1 = 0.1 + 1 \quad H/D_1 = 2 + 10$$

Sketch of the configuration conductor-windows

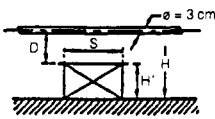


$$K = 1.25 + 0.005 \left( \frac{H}{D} - 6 \right) + 0.25 (e^{-8 S/D} - 0.2)$$

Applicable in the range:

$$D = 2 + 10 \text{ m}, S/D = 0.1 + 1, H/D = 2 + 10 \quad K = 1.25$$

Sketch of the configuration conductor-lower structures



$$K = 1.15 + 0.81 \left( \frac{H'}{H} \right)^{1.167} + 0.02 \frac{H'}{D} - A \left[ 1.209 \left( \frac{H'}{H} \right)^{1.167} + 0.03 \left( \frac{H'}{H} \right) \right] (0.67 - e^{-2 S/D})$$

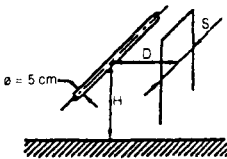
where  $A = 0$  if  $S/D < 0.2$  and  $A = 1$  if  $S/D \geq 0.2$ .

Applicable in the range:

$$D = 2 + 10 \text{ m}, S/D = 0 + \infty, H'/H = 0 + 1$$

$K = 1.15$   
for cond-  
plane to 1.5  
or more

Sketch of the configuration & conductor-lateral structures



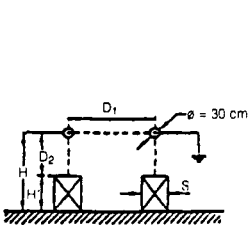
$$K = 1.45 + 0.024 \left( \frac{H'}{H} \right) - 6 + 0.35 (e^{-8 S/D} - 0.2)$$

Applicable in the range:

$$D = 2 + 10 \text{ m}, S/D = 0.1 + 1, H/D = 2 + 10$$

$K = 1.45$

Sketch of the configuration cross & rod-rod-structures (open switchgear)



$$K_1 = 1.35 - 0.1 \frac{H'}{H} - \left( \frac{D_1}{H} - 0.5 \right)$$

Rod-lower structure

$$K_2 = 1 + 0.6 \frac{H'}{H} - A 1.093 \frac{H'}{H} (0.549 - e^{3 S/D}) \quad K_1 = 1.3$$

where  $A = 0$  if  $S/D_2 < 0.2$  and  $A = 1$  if  $S/D_2 \geq 0.2$ .

Applicable in the range:

$$(K_1) D_1 = 2 + 10 \text{ m} \quad D_1/H = 0.1 + 0.8 \quad D_1 < D_2 \quad 0.6 \frac{H'}{H} \\ (K_1) D_2 = 2 + 10 \text{ m} \quad S/D_2 = 0 + \infty \quad D_2 < D_1$$

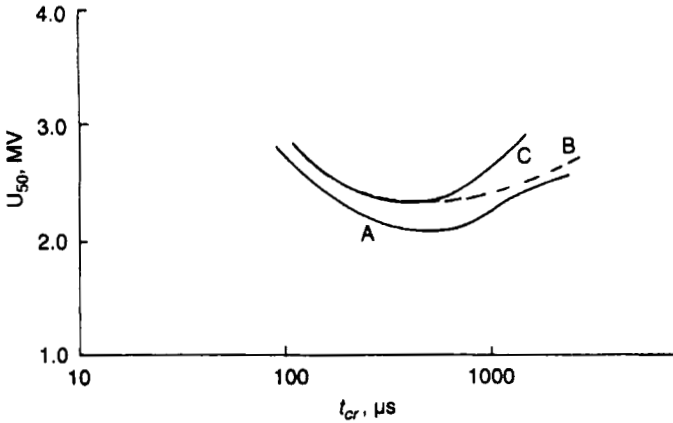


Figure 20.4 U-curves for 13 m positive rod-plane, sphere-plane and conductor-plane gaps (after [4]). Gap factors as follows:

$T_{cr}, \mu s$	R-P (A)	S-P (B)	C-P (C)
100	1.00	1.07	1.07
200	1.00	1.10	1.10
500	1.00	1.12	1.10
1000	1.00	1.07	1.19
1100	1.00	1.04	1.23

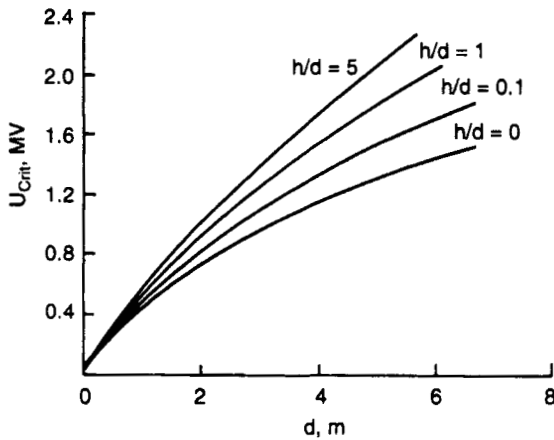


Figure 20.5 Rod-rod positive switching impulse sparkover characteristics as function of height  $h$  of lower rod above ground plane. Positive polarity to upper rod (after [5])

$h/d$	Gap factor ( $d = 3$ m)
0	1 (rod-plane)
0.1	1.15
1.0	1.32
5.0	1.46

breakdown characteristics. Figure 20.6 presents the results of a study in a rod-rod gap in which an earthed metal plane was placed parallel to the axis of a rod-rod system, at a distance 14% greater than the electrode separation [7]. The same study showed that the proximity of such an earth plane to a rod-plane gap of similar range of dimensions had a very much smaller effect than in the case of the rod-rod gap.

## 20.5 Sparkover characteristics

### 20.5.1 Test procedures

The variability in the pre-breakdown processes summarised in Section 20.2 results in a variability in sparkover voltage, particularly when impulse voltages are used. It is necessary therefore to devise an average sparkover voltage to describe the strength of a particular gap. For this purpose the  $U_{50}$  or 50% sparkover voltage, is used – this is the impulse crest voltage at which there is a probability of 0.5 that the gap will spark over. With impulse voltages, it can be determined in two ways: (a) the variable voltage method and (b) the ‘up-and-down’ method [7, 8].

In method (a) an estimate of the likely value of  $U_{50}$  is made, either from experience or by means of a few trial shots and several sets of, say, 20 impulses each at constant crest voltage, which may then be applied to the gap. The voltage levels of the sets may differ from one another by the order of 1% of  $U_{50}$ . Each set of 20 yields a probability of sparkover at the voltage used. The probabilities are plotted against voltage on normal probability paper and an approximate straight line is usually obtained.  $U_{50}$  is then immediately determined.

Method (b) is more economical in the number of impulses required. The voltage is raised, around the estimated  $U_{50}$ , in constant steps of 2 or

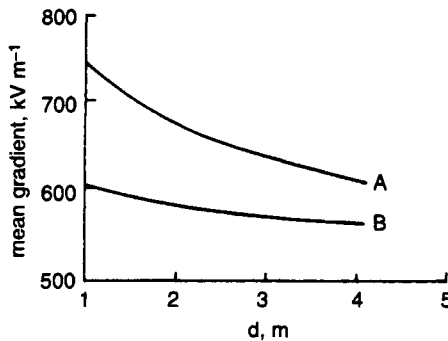


Figure 20.6 Rod-rod sparkover characteristics with earthed metal plane in proximity, expressed as mean gradient,  $kVm^{-1}$   
A without plane, B with plane

3% of this value, until a sparkover takes place. It is then lowered by one step. If no sparkover occurs, it is raised again and this procedure is repeated, raising or lowering according to the result occurring in the preceding impulse. After a number of impulses, usually less than about 50, a voltage is reached which is very close to  $U_{50}$ . This technique can be made more precise if, after completion of the foregoing procedure, groups of 50 shots are tried at the estimated  $U_{10}$  and  $U_{90}$  conditions. If the results so obtained are plotted with the rest of the data, a value of  $U_{50}$  can be determined with very little uncertainty.

Each of these methods implicitly assumes a relation between the probability  $p$  of sparkover and a voltage  $U$  of the Gaussian form:

$$p = \frac{1}{(\sqrt{2} \pi S)} \int_0^U \exp - \frac{(U - U_{50})^2}{S^2} dU \quad (20.5)$$

where  $S$  is the variation in  $U$  between  $U_{50}$  and the value of  $U$  at which  $p$  is either 0.16 or 0.84. It is this value of  $S$  that is commonly quoted in describing the deviation about  $U_{50}$  in practical tests. Values of the order of 5% are common under switching impulses.

This assumption of a normal, or Gaussian, distribution has proved adequate for most test purposes, but more painstaking investigations [9] have shown that the probability distributions can sometimes be far from normal.

When alternating voltages are being measured, the sparkover voltage depends on the time for which the voltage is applied; it can decrease by up to 10% for an application of voltage to the test gap which is rising for periods up to 1000  $\mu$ s. It is therefore necessary to specify, for a given test, the rate at which the voltage rise takes place.

Similar considerations apply in the case of direct voltages. Here, for instance, the IEC [8] lays down that the voltage shall be raised to the breakdown value in approximately 1 min, with a rate of rise of  $\approx 1\%/s$  in the final stages. The scatter in sparkover values, expressed as a standard deviation, is usually less than 1%, where the more highly stressed electrode is positive.

## 20.5.2 *Sparkover voltage characteristics*

### 20.5.2.1 *Impulse conditions: rod-plane gaps*

The practical engineer is faced with a variety of possible electrode geometries, but we have seen that the rod-plane gap forms a valuable reference. Jones and Waters [10] have presented a summary showing the mean breakdown gradient  $U_{50}/d$  against gap length for this gap; it is reproduced here as Figure 20.7. Results for alternating and direct voltages are also included here.

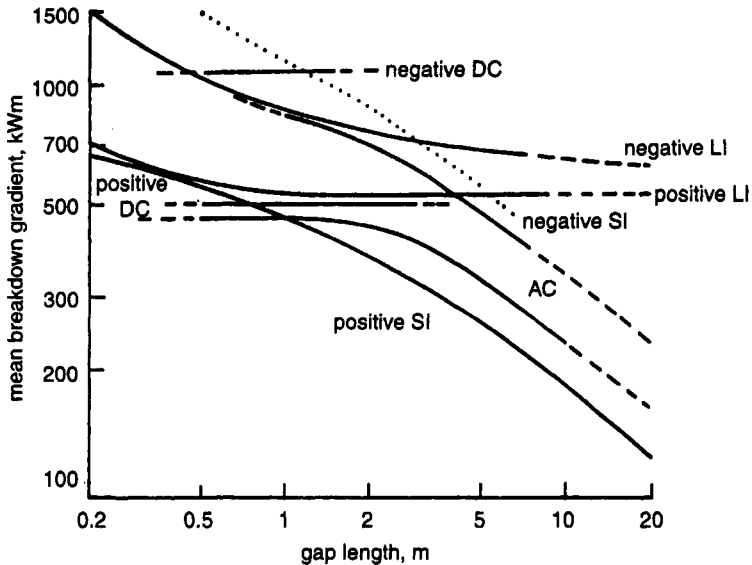


Figure 20.7 Mean breakdown gradient of rod-plane gaps under standard atmospheric conditions as a function of gap length for different testing waveforms [10]

A further important reference condition becomes apparent. For the positive lightning impulse, the mean gradient remains constant, for gap lengths greater than about 1 m, at  $\approx 500 \text{ kV m}^{-1}$ . This is approximately the same as the streamer gradient  $E_s^+$  (Section 20.2 and eqn (20.4)), a fact that is utilised in the IEC atmospheric correction procedures (Section 20.6). Thus, the sparkover voltage  $U_{50}$  increases linearly with gap length. For the negative lightning impulse, the gradient is higher but is not constant with gap; the sparkover voltage increases with electrode spacing less rapidly than linearly. No simple explanation can be offered here, if only because negative polarity has been studied much less than positive; the reason for this is that the higher gradients make negative impulses less dangerous to power systems than positive impulses.

Under positive switching impulse, the gradient declines with increasing gap length, due to the increasing growth of the low-gradient leader channel. The breakdown strength depends only on the gap length and is often expressed by the formula [4]:

$$U_{50(\text{crit})} = \frac{3400}{(1 + 8/d)} \quad \text{kV} \quad (20.6)$$

where  $U_{50(\text{crit})}$  is the value of  $U_{50}$  at the critical time to crest, that is, the minimum value. This expression holds over the range of gaps  $2 \text{ m} < d < 15 \text{ m}$ .

Figure 20.7 shows that the positive switching impulse characteristic becomes more linear for gap lengths > 10 m and a more appropriate relationship is the following:

$$U_{50(crit)} = 1400 + 55d \quad \text{kV} \quad (20.7)$$

The following formula has also been proposed [4] as being reasonably accurate for all gaps up to 25 m:

$$U_{50(crit)} = 1080 \ln(0.46d + 1) \quad \text{kV} \quad (20.8)$$

Finally, for the particular case of the IEC standard positive switching impulse, that is 250/2500  $\mu\text{s}$ , the value of  $U_{50}$  (which is not now at a critical time-to-crest) is well described by

$$U_{50} = 500 d^{0.6} \quad \text{kV} \quad (20.9)$$

Under negative switching impulses, the following relationship holds with reasonable precision over the range  $2 \text{ m} < d < 14 \text{ m}$  [4]:

$$U_{50(crit)} = 1180 d^{0.45} \quad \text{kV} \quad (20.10)$$

Figure 20.8 compares practical values with some of these relationships [4].

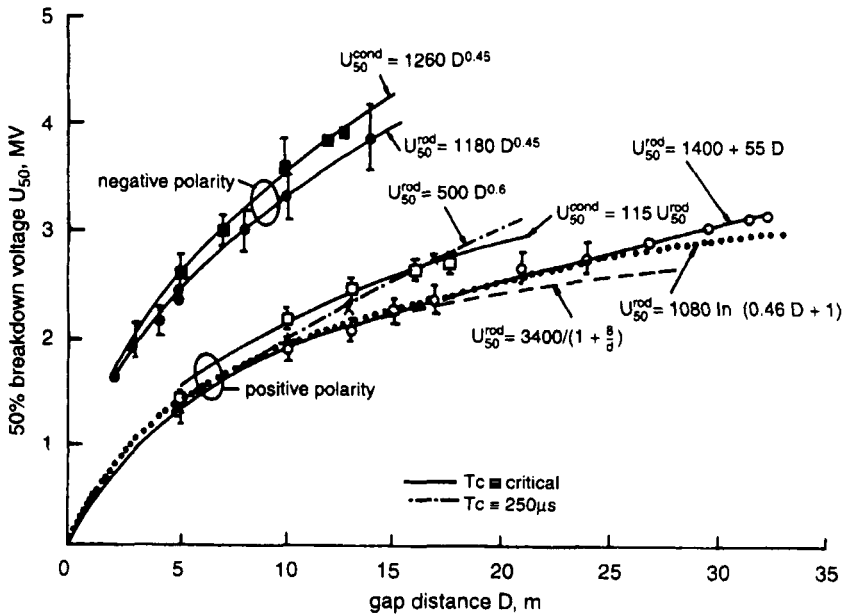


Figure 20.8 Switching impulse characteristics for long gaps. Rod-plane and phase conductor-plane (after [4])

20.5.2.2 Airgaps of other shapes

The expressions (20.6) and (20.7) can, in principle, be applied to gaps of more practical interest, provided the RHS of each is multiplied by the gap factor  $K$ . This statement must, of course, be qualified by the reservations already discussed in Section 20.4.

Figure 20.9, reproduced from [10], summarises the available information on the minimum flashover mean gradients, that is, at critical time-to-crest, for a variety of gaps. Again, it will be noted that gradients are higher when the highly stressed electrode is negative rather than positive.

20.5.2.3 Sparkover under alternating voltages

Here again, the rod-plane gap exhibits the lowest sparkover voltage and the 50% breakdown condition is given by [11]

$$U_{50} = 750 \ln(1 + 0.55d^{1.2}) \quad \text{kV} \quad (20.11)$$

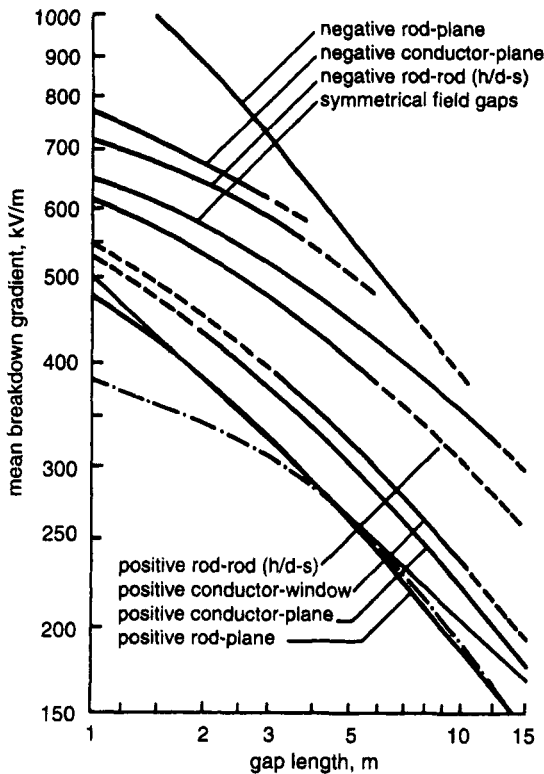


Figure 20.9 Minimum 50% sparkover gradient as a function of gap length for various reference geometries [10]

for values of  $d$  greater than 2 m. To give perspective, it may be noted that the peak values of  $U_{50}$  are of the order 20% higher than those for switching impulses of critical time-to-crest for the same gap.

For estimation of the flashover voltage of gaps other than the rod-plane, it has become customary to use the gap-factor  $K$  for switching impulses. This procedure is clearly subject to the same limitations as have been outlined already, but the following equation has been given [11]:

$$U_{50} = U_{50}(rp) (13.5K - 0.35K^2) \quad \text{kV RMS} \quad (20.12)$$

For gaps in the range  $2 \text{ m} < d < 6 \text{ m}$  this formula holds to within  $\pm 10\%$  for most of the following gaps: conductor-plane, conductor-structure (underneath), conductor-structure (lateral), rod-rod, conductor-rod, conductor-rope [12]. As noted earlier, flashover voltages are influenced by the rate of increase of voltage, with a decrease of up to 5% for slow rates of rise of voltage towards breakdown of the order of 1 h.

#### 20.5.2.4 *Sparkover under direct voltages*

In positive rod-plane gaps in the range  $0.5 \text{ m} < d < 5 \text{ m}$ , direct voltage sparkover voltages increase linearly with gap length, with a mean gradient of the order of  $500 \text{ kVm}^{-1}$  [13, 14]. This characteristic is similar to that of the rod-plane gap under lightning impulse. In both cases, linearity is due to the dominance of the streamer pre-discharge, but in the positive direct voltage case, the reproducibility of sparkover voltage is greater, the standard deviation being less than 1%.

For the negative rod-plane gap, the gradient is higher, of the order of  $1000 \text{ kVm}^{-1}$  with a slight tendency for the flashover voltage to increase less rapidly than linearly in gaps larger than 1 m in length [15]. Gap factors for gaps other than rod-plane, and derived from direct voltage measurements, are given in Table 20.3.

*Table 20.3 Gap factors under direct voltages (data from [11])*

Configuration	Gap $d$ , m	Sparkover voltage, kV	Gap factor
Rod-plane	1	450	1
	2	910	1
Rod-rod*	1	520	1.16
	2	1050	1.15
Single conductor-structure	1	600	1.33
	2	1150	1.26
Bundled (4) conductor-structure	1	460	1.02
	2	950	1.04

\* Tip of lower-rod 1.5 m above ground plane

The rod-rod gap has proved of particular use as a tool for the measurement of direct voltage, since it retains the property of linearity up to  $d = 3$  m [8] and, provided it is mounted well above the ground plane, possesses the same characteristics whatever the polarity of the voltage being used. It has now been adopted by the IEC as a secondary standard for the measurement of direct voltages.

#### *20.5.2.5 Flashover across insulator surfaces in air*

The weakest aspect of the insulation of high-voltage systems is frequently the dielectric strength of the surface of the solid insulator which is used to separate the conductors. Knowledge of the basic processes involved is still relatively fragmented, but it is known that streamers, once initiated, may travel more rapidly across certain insulator surfaces in air than they do in the air in the absence of the insulator, and it is known that charges deposited on the surface by corona may so alter the electric field distribution as to facilitate breakdown. However, in practice, other factors may likewise cause field distortions and encourage breakdown: unequal distribution of capacitance between insulators; stray capacitances to ground; field concentration at the 'triple junction' between insulator, conductor and air; layers of pollution; rain and deposition of moisture – all of these can contribute to weakness in the dielectric strength of a surface.

The tendency of a surface to reduce the insulation strength is minimised by the adoption of 'sheds' to increase the total length of path between conductors. The 'cap and pin' insulator takes this concept to the limit and almost all power lines operating at above 100 kV use strings of insulators of this type. The deep sheds ensure that discharges must cover most of their path in the air and tests have shown [16] that the loss of dielectric strength, compared with that in air, is not usually more than about 3% under impulse voltages. This result is true for conductor-tower cross-arm situations, for both polarities, but larger polarity differences may arise when a configuration such as rod-plane, with insulators, is tested. Indeed, when negative impulse voltages are applied to the highly stressed electrode, results which are very sensitive to the electrode profile may be obtained; this is because high field concentrations at the 'triple junction' may set up a cathode mechanism which encourages the initiation of discharges.

## **20.6 Atmospheric effects**

All that has been written in the preceding sections must be qualified by the realisation that in air, the temperature, pressure and humidity change in an uncontrolled way. It is necessary, therefore, to establish procedures

by which (a) it is possible to estimate flashover voltages at any atmospheric condition from those measured at another condition, and (b) measurements can be corrected to a standard atmospheric condition for the purposes of comparison of results obtained in different laboratories at different times.

### 20.6.1 *Density effects*

Temperature and pressure together determine the density of the air. The ionisation processes involved in corona and breakdown depend primarily on the air density and not, to any significant degree, specifically on temperature except insofar as it changes density. Moreover, many experiments have shown that over limited ranges of density, breakdown voltages vary linearly with density. Thus, it has proved a relatively straightforward matter to define a set of conditions that can be regarded as characteristic of a standard atmosphere, and to relate other conditions of pressure and density to the standard atmosphere, assuming the simple gas laws to be correct. A standard atmosphere is defined for these purposes as at 101.3 kPa (760 torr) and 293 K (20 °C). Then, at any temperature  $T$  and pressure  $p$ , the density has changed from that at the standard atmosphere by

$$\delta = \frac{p}{1013} \frac{293}{T} \quad (20.13)$$

and clearly the value of  $\delta$  is the ratio of the density at  $(p, T)$  to that at the standard condition.  $\delta$  is called the relative air density;  $\delta = 1$  at the standard condition.

If, now, the value of  $U_{50}$  at relative air density  $\delta = 1$  is denoted by  $U_0$ , then the value  $U$  at  $(p, T)$  is given by

$$U = U_0 \delta \quad (20.14)$$

It should be observed here that this discussion has ignored any effects due to change of humidity. These effects will be discussed below, but it should be noted that the standard atmospheric condition assumes an absolute humidity of 11 g moisture content per cubic metre of air.

Over the normal extreme range of temperatures encountered in practice, that is, between 313 K and 243 K approximately, the density correction procedure has been judged satisfactory. Values and curves of flashover voltages presented in the literature are usually described as uncorrected or, alternatively, corrected to  $\delta = 1$ , in the latter case so enabling comparisons to be made. The procedure is used for impulse, alternating and direct voltage measurements.

The procedure has also proved satisfactory for normal variations of

pressure at altitudes up to 2000 m, but evidence has accumulated showing that at greater altitudes (lower pressures) the linearity breaks down and a modified procedure must be used [17].

### 20.6.2 Humidity effects

Atmospheric humidity can change from a moisture content of less than  $1 \text{ gm}^{-3}$  in very cold countries to the order of  $30 \text{ gm}^{-3}$  in the tropics. The effects of humidity on sparkover are quite complex, but the following general points can be made:

- (a) Humidity has its strongest influence on the positive pre-breakdown discharge. In particular, the streamer gradient  $E_s^+$  (eqn (20.1)) increases at the rate of roughly 1% per  $\text{gm}^{-3}$  increase in moisture content.
- (b) Humidity has no significant effect on the leader gradients  $E_l^+$  and  $E_l^-$ , though it does have the effect of increasing the leader velocity.
- (c) Humidity has no significant effect on the negative sparkover under lightning impulse and under direct voltages.

A rough general rule therefore follows from (a), (b) and (c): where a sparkover is preceded only by positive corona, there is a significant humidity influence, but where it is preceded only by negative corona, there is no significant effect. Thus, for instance, under lightning impulse, humidity shows a maximum effect on sparkover in the positive rod-plane gap but no effect in the negative rod-plane gap.

The effects of humidity on sparkover have been widely studied and have led to a correction procedure which uses the IEC curves shown in Figure 20.10. Here  $k$  is a factor by which a sparkover voltage at a standard humidity  $h$  of  $11 \text{ gm}^{-3}$  must be multiplied to estimate what its value would be at any other humidity. Note that the abscissa here is in fact  $h/\delta$ , where  $\delta$  is the relative air density; this usage arises from the fact that a given partial pressure of water vapour makes up a varying proportion of the air moisture as the density changes. A brief account of practical cases is now given.

Under positive lightning impulse, we have seen that sparkover is determined substantially by the streamer gradient  $E_s^+$  and this is reflected in the expression for  $k$ , given in Figure 20.10 where, for impulse voltage the rate of change with  $h/\delta$  is 0.01, or 1% per  $\text{gm}^{-3}$ . The correction procedure holds very well in this case. Where a switching impulse is used, Figure 20.10 must be used with care, for substantial leader growth occurs and we have seen in (b) above that humidity has little influence on the leader gradient. Thus the rate of change of  $k$  with  $h/\delta$  falls appreciably below 0.01 when the leader has traversed a significant part of the gap prior to sparkover. Also, since the leader velocity increases with humidity it is found that the minimum of the U-curve shifts towards lower times-to-crest; this is

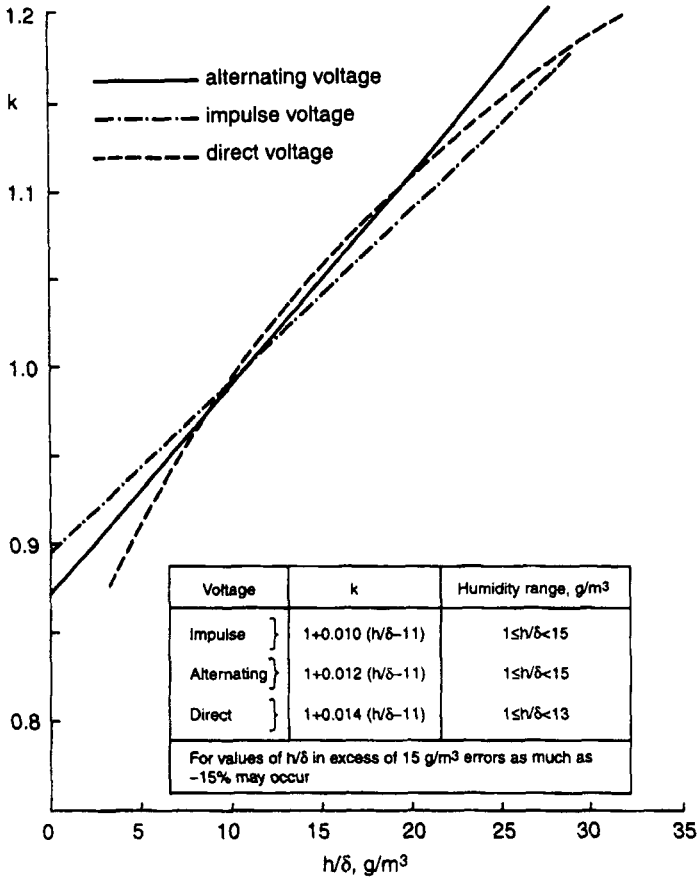


Figure 20.10 IEC curves and expressions for humidity correction procedure

shown clearly in Figure 20.2. In such cases, it is best to determine humidity influence by practical tests where possible.

Under direct voltages, sparkover is again determined substantially by streamer growth and the correction procedure holds very well with a rate of change of  $k$  with  $h/\delta$  of 0.014 or 1.4% per  $\text{g/m}^3$ . There is an important limitation, however, for gaps of the order of 1 m or greater and for humidities greater than  $\approx 13 \text{ g/m}^3$ . Here the linearity between sparkover voltage and electrode spacing breaks down and, again, it is advisable to check humidity influence by practical tests where possible.

Under alternating voltages, application of the correction procedure is very difficult and it has been shown that at moderate humidities, around  $13 \text{ g/m}^3$ , the sparkover voltage can become very variable [18]. The effects of humidity on alternating voltage sparkover have been studied least of all and there are many uncertainties that remain to be resolved.

A full account of humidity effects and problems is given in [19].

### 20.6.3 Other atmospheric effects

High voltage power systems must contend with atmospheric pollution, rain, ice and snow and occasionally forest fires beneath overhead lines. The first three of these have their greatest effects on insulators, as indeed does the fourth, by deposition of soot, etc. The last mentioned also has drastic local effects on air density, which may result in sparkovers.

Detailed discussion of these topics is beyond the scope of this chapter; further information can be found in References [20, 21, 22].

## 20.7 New developments

There is interest in the subject of 'line compaction' of overhead lines in large-scale power systems, to reduce both costs and the visual impact on the environment. This will require a re-appraisal and an extension of measurements of sparkover characteristics in gaps of various geometries, with emphasis on the low-level probabilities of sparkover. Live-line working is also an issue at the present time, and studies of the influence of perturbing factors such as tools, floating objects and men working on lines on sparkover voltages and clearances between conductors are being undertaken in several countries. Finally, the efficacy of nonceramic and composite insulators, as alternatives to the traditional ceramic or glass insulators, is under discussion and their flashover characteristics require study.

## 20.8 References

- 1 BÜSCH, W.: 'Air humidity, an important factor of UHV design', *IEEE Trans.*, 1977, **PAS-91**, (6), pp. 2086–2093
- 2 PARIS, L. and CORTINA, R.: 'Switching and lightning impulse discharge characteristics for large air gaps and long insulator strings', *IEEE Trans.*, 1968, **PAS-98**, pp. 947–957
- 3 Les Renardières Group: 'UHV air insulation: physical and engineering research', *Proc. IEE*, 1986, **133-A**, pp.438–468
- 4 HUTZLER, B., GARBAGNATI, E., LEMKE, E. and PIGINI, A.: 'Strength under switching overvoltages in reference ambient conditions', in: CIGRÉ Working Group 33.07, 'Guidelines for the evaluation of the dielectric strength of external insulation' (CIGRÉ, Paris, 1993)
- 5 DIESENDORF, W.: 'Insulation coordination in high voltage electric power systems' (Butterworth, London, 1974)
- 6 GALLIMBERTI, I. and REA, M.: 'Development of spark discharges in long rod-plane gaps under positive impulse voltages', *Alta Freq.*, 1973, **42**, pp. 264–275
- 7 STANDRING, W.G., BROWNING, D.N., HUGHES, R.C. and

- ROBERTS, W.J.: 'Impulse flashover of air gaps and insulators in the voltage range 1–2.5 MV', *Proc. IEE*, 1963, **110**, (6), pp. 1082–1088
- 8 IEC 60060-1 (1989): 'High voltage test techniques, Part 1: General definitions and requirements'
  - 9 MENEMENLIS, C. and HARBEC, G.: 'Particularities of air insulation behaviour', *IEEE Trans.*, 1976, **PAS-95**, pp. 1814–1821
  - 10 JONES, B. and WATERS, R.T.: 'Air insulation at large spacings', *Proc. IEE*, 1978, **125**, (11R), pp. 1152–1176
  - 11 PIGINI, A., THIONE, L. and RIZK, F.: 'Dielectric strength under AC and DC voltages,' in: CIGRÉ Working Group 33.07 'Guidelines for the evaluation of the dielectric strength of external insulation' (CIGRÉ, Paris, 1993)
  - 12 CORTINA, R., MARRONE, G., PIGINI, A., THIONE, L., PETRUSCH, W. and VERMA M.P.: 'Study of the dielectric strength of external insulation of HVDC systems and application to design and testing,' CIGRÉ, 1984, Paper 33-12
  - 13 FESER, K. and HUGHES, R.C.: 'Measurements of direct voltages by rod-rod gap', *Electra*, 1988, **64**, (117), pp. 23–35
  - 14 BOUTLENDJ, M., ALLEN, N.L., LIGHTFOOT, H.A. and NEVILLE, R.B.: 'Transitions in flashover characteristics of rod-plane gaps under positive direct voltage in humid air'. *Proc. 7th Int. Symp. on High voltage engineering*, Dresden, Paper 42.17, 1992
  - 15 KNUDSEN, N. and ILICETO, F.: 'Flashover tests on large air gaps with DC voltage and with switching surges superimposed on DC voltage', *IEEE Trans.*, 1970, **PAS-89**, pp. 781–788
  - 16 HUTZLER, B. and RIU, J.P.: 'Behaviour of long insulator strings in dry conditions', *IEEE Trans.*, 1979, **PAS-98**, (3), pp. 982–991
  - 17 MORENO, M., PIGINI, A. and RIZK, F.: 'Influence of air density on the dielectric strength of air insulation,' in: CIGRÉ Working Group 33.07. 'Guidelines for the evaluation of the dielectric strength of external insulation' (CIGRÉ, Paris, 1993)
  - 18 FESER, K.: 'Influence of humidity on the breakdown characteristics under AC voltage', *ETZ*, 1970, **91**, (10)
  - 19 ALLEN, N.L., FONSECA, J., GELDENHUYS, H.J. and ZHENG, J.C.: 'Humidity influence on non-uniform field breakdown in air', *Electra*, 1991, **134**, pp. 63–90
  - 20 LEMKE, E., FRACCHIA, A., GARBAGNATI, E. and PIGINI, A.: 'Performance of contaminated insulators under transient overvoltages. Survey of experimental data,' in: CIGRÉ Working Group 33.07, 'Guidelines for the evaluation of the dielectric strength of external insulation' (CIGRÉ, Paris, 1993)
  - 21 KAWAMURA, T. and NAITO, K.: 'Influence of ice and snow' in: CIGRÉ Working Group 33.07, 'Guidelines for the evaluation of the dielectric strength of external insulation' (CIGRÉ, Paris, 1993)
  - 22 FONSECA, J., SADURSKY, K., BRITTEN, A., MORENO, M. and VAN NAME, J.: 'Influence of high temperature and combustion particles (Presence of fires)' in: CIGRÉ Working Group 33.07, 'Guidelines for the evaluation of the dielectric strength of external insulation' (CIGRÉ, Paris, 1993)